

**PETROPHYSICAL ANALYSIS OF MIANO-09 WELL,
LOWER INDUS BASIN, PAKISTAN**



A thesis submitted to Bahria University, Islamabad in partial fulfillment
of the requirement of the degree of B.S in Geology

Muhammad Awais

Umer Azam

Usama Aman Ullah



Department of Earth and Environmental Sciences

Bahria University, Islamabad, Pakistan

2020




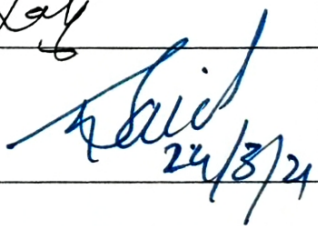
Bahria University

Department of Earth & Environmental Sciences
Islamabad Campus, Islamabad

Dated: 17/03/2021

Certificate

A thesis submitted by **Mr. Umer Azam, Mr. Muhammad Awais and Mr. Usama Aman Ullah** to the Department of Earth & Environmental Sciences, Bahria University, Islamabad in partial fulfillment of the requirements for the degree of **Bachelor in Geology** (Session 2016–2020).

Committee Member	Name	Signature
Supervisor	Mr. Saqib Mehmood	
Internal Examiner	Mr. Mumtaz Ali Khan	
External Examiner	Dr. Saiq Shakeel Abbasi	
Head of Department (E&ES)	Dr. Said Akbar Khan	 24/3/24



ABSTRACT

The objective of this study is to determine the hydrocarbon potential in Miano-09 well using wireline logs. Miano Gas field is located in the Thar Desert, in the Sukkur region. Log data used in this study includes the Gamma-ray log, Gamma ray Neutron tool, Resistivity log, Caliper log, and SP log. The borehole profile of the zone of interest was good. The calculation of the porosity was carried out with the help of the Gamma-ray Neutron Tool. One prospect zone had been marked within B interval. The present study showed that the volume of clean was about 90.56%. The total porosity of the zone of interest was 3.12% while effective porosity was 12.02%. Saturation of water was 41.37% which showed that the zone of interest is a hydrocarbon-bearing zone as compared to water. Petrophysical analysis showed that prospect zone has clean lithology and good effective porosity. Beside clean lithology and good effective porosity there is relatively high percentage of hydrocarbon saturation. Therefore, petrophysical analysis reveal that in Miano-09, B-interval of Lower goru formation is acting as an effective reservoir.

ACKNOWLEDGMENTS

Above all else, it is of most extreme hugeness to bow our head before Allah Almighty who is the Mightiest and all Gracious. He made us ready to finish this thesis work effectively. Endless greetings are upon the Holy Prophet Muhammad (S.A.W.W), the establishment of knowledge who consistently guided His Ummah to seek information or knowledge. After that, we are appreciative of our cherished guardians that their all the best, petitions and unqualified love reinforce us to accomplish our objective. We are obliged to our noteworthy supervisor senior Assistant Mr. Saqib Mehmood, Senior Assistant Professor, Department of Earth and Environmental Sciences, Bahria University, Islamabad for his master direction, nonstop support, and dedication all through our research work.

Our assertion of much gratitude goes to Dr. Said Akbar Khan, Head of Department, of Earth and Environmental Sciences, Bahria University, Islamabad for their help and concern. We are additionally appreciative of Mr. Adeeb Ahmed, Lecturer, Bahria University, Islamabad for his help and participation with us in completing this research work.

CONTENTS

ABSTRACT	i
ACKNOWLEDGMENTS	ii
FIGURES	vi
TABLES	vii
ABBREVIATIONS	viii

CHAPTER 1

INTRODUCTION

1.1.	Introduction of area	1
1.2.	Exploration History	1
1.3.	Objectives	2
1.4.	Methodology	3

CHAPTER 2

GEOLOGY AND TECTONICS

2.1.	Regional tectonic setting of Pakistan	4
2.2.	Geological setting	6
2.2.1.	Basin architect of Miano and adjoining areas	6
2.3.	Nomenclature of lower goru sands	8
2.4.	Generalized stratigraphy of lower Indus basin	8
2.4.1.	Siwalik Member	9
2.4.2.	Kirthar formation	9
2.4.3.	Drazinda Formation	10
2.4.4.	Pirkoh member	10
2.4.5.	Sirki member	10
2.4.6.	Habib Rahi formation	11
2.4.7.	Ghazij member	11
2.4.8.	Laki Formation	11

2.4.9.	Sui main limestone	12
2.4.10.	Ranikot formation	12
2.4.11.	Parh Limestone	12
2.4.12.	Goru formation	13
2.5.	Petroleum System of lower Indus basin	14
2.5.1.	Source Rock	14
2.5.2.	Reservoir Rock	14
2.5.3.	Seal Rock	15
2.5.4.	Traps	15
2.6.	Bore-hole stratigraphy	16
2.7.	Petroleum play	17

CHAPTER 3

PETROPHYSICAL ANALYSIS

3.1.	Introduction	18
3.2.	Methodology	18
3.3.	Log Trends of Miano-09 well	19
3.4.	Data used	20
3.4.1.	Calliper Log	20
3.4.2.	Gamma Ray (GR) Log	20
3.4.3.	Spontaneous potential (SP) Log	21
3.4.4.	Resistivity log	21
3.4.5.	Bulk Density Log	22
3.4.6.	Neutron log	22
3.5.	Zone Of interest	23
3.6.	Petrophysical analysis of Miano-09 well	23
3.6.1.	Calculating Volume of Shale (Vsh)	23
3.6.2.	Calculating Neutron porosity	25

3.6.3. Calculating Density porosity (DPHI)	25
3.6.4. Calculating Effective porosity (EPI)	26
3.6.5. Resistivity of water	27
3.6.6. Saturation of water and saturation of hydrocarbons	32
3.7. Result	35
CONCLUSION	36
REFERENCES	37
APPENDIX	38

FIGURES

Figure 1.1. Location map of study well (Arc GIS 10.5)	2
Figure 1.2. Flow chart displaying methodology adopted in the present study	3
Figure 2.1. Regional tectonic setting of Pakistan	5
Figure 2.2. Tectonic map of study area	7
Figure 2.3. Nomenclature of lower goru sands	8
Figure 2.4. Stratigraphy of lower indus basin	13
Figure 3.1. Log trend showing depth interval of zone of interest(3338m-3345m)	19
Figure 3.2. Cross plot showing volume of shale and volume of clean against depth	24
Figure 3.3. Relation between Vshale and porosities	27
Figure 3.4. Conversion of $RMF@S.T$ to $RMF@F.T$ using Gen-9 chart	29
Figure 3.5. Conversion of Rmf to Rmfeq using SP-2 chart	30
Figure 3.6. Conversion of SSP and Rmfeq to Rweq using SP-1 chart	31
Figure 3.7. Conversion of Rweq to Rw using SP-2 chart	32
Figure 3.8. Cross plot between the saturation of water and hydrocarbons	34

TABLES

Table 2.1. Borehole stratigraphy of Miano-09 well.	16
Table 2.2. Petroleum play of Miano-09 well.	17
Table 3.1. Zone of interest in Miano-09 well	23
Table 3.2. The average volume of shale and the average volume of clean	25
Table 3.3. Average neutron porosity	25
Table 3.4. Average density porosity	26
Table 3.5. Average Effective porosity	27
Table 3.6. Average hydrocarbons and water saturation in %	34
Table 3.7. Summary of different petrophysical parameters	35

ABBREVIATIONS

R _{mc}	Resistivity of Mud Cake
R _{mf}	Resistivity of Mud Filtrate
R _m	Resistivity of Mud
R _{xo}	Resistivity of Flushed Zone
R _t	Resistivity of True Zone
R _w	Resistivity of Water
R _{mfeq}	Equivalent Mud Filtrate Resistivity
R _{weq}	Equivalent Formation Water Resistivity
S _h	Saturation of Hydrocarbons
S _w	Saturation of Water
D _i	Diameter of Invaded Zone
D _h	Diameter of Borehole
G.G	Geothermal Gradient
S.T	Surface Temperature
B.H.T	Bottom Hole Temperature
SPDZ	South Potwar Deformed Zone
NPDZ	North Potwar Deformed Zone
MMBBL	Million Barrels Oil
MMCFD	Million Cubic Feet per Day
BOPL	Barrel of Oil per Day
V _{sh}	Volume of Shale
V _{clean}	Volume of Clean

CHAPTER 1

INTRODUCTION

1.1 Introduction of area

The Miano gas field is the key discovery of a natural gas reservoir generated in 1993 by OMV (Pakistan). This gas field is situated in the Thar Desert, in the Sukkur region. In Mubarak block, Miano field was discovered and is the first known stratigraphic trap found in Pakistan. A joint venture between OMV Exploration (Pakistan), ENI Exploration and Production Limited (Italy), Pakistan Petroleum Limited (PPL) and Oil and Gas Development Company Limited is the field under consideration (Miano) in the Sindh Province of Pakistan (OGDCL). To date, production has been obtained from seven of the eighteen wells penetrated in the area. (Raza et al., 2020, pp. 18-19)

The Miano region lies 62 kilometers southeast of Sindh, Pakistan's city of Sukkur. Nearly 42km adjacent to the strike, it lingers. The Miano-09 well has 027.371747 latitude and 069.311478 longitude. The location of the Miano-09 well is shown in figure 1.1.

1.2 Exploration History

The two productive fields of Pakistan, the Mari and Sui gas fields, are separately located 75 km and 150 km north of the Miano site. Until now, the eight wells were penetrated in the B-Interval of the Lower Cretaceous Goru Formation. The reservoir examination region faces north to the Middle Eastern Ocean with the Kohat-Potwar platform to the north remains surrounded, mainly north-south drifting Indus Basin. The fold and fault belts of the Sulaiman and Kirthar ranges face this area on the eastern side.

The area is situated along the western margin of the Indian Plate in the Central Indus Basin (CIB), bordered by two regional peaks, i.e. the Mari-Kandhkot High to the northeast and the Jacobabad-Khairpur High to the southwest. The CIB is a gas prone province comprising 70% of Pakistan's identified gas reserves. In the Upper

Cretaceous and Tertiary rivers, confirmed deposits are locked dominantly. (Kadri, I.B, 1995)

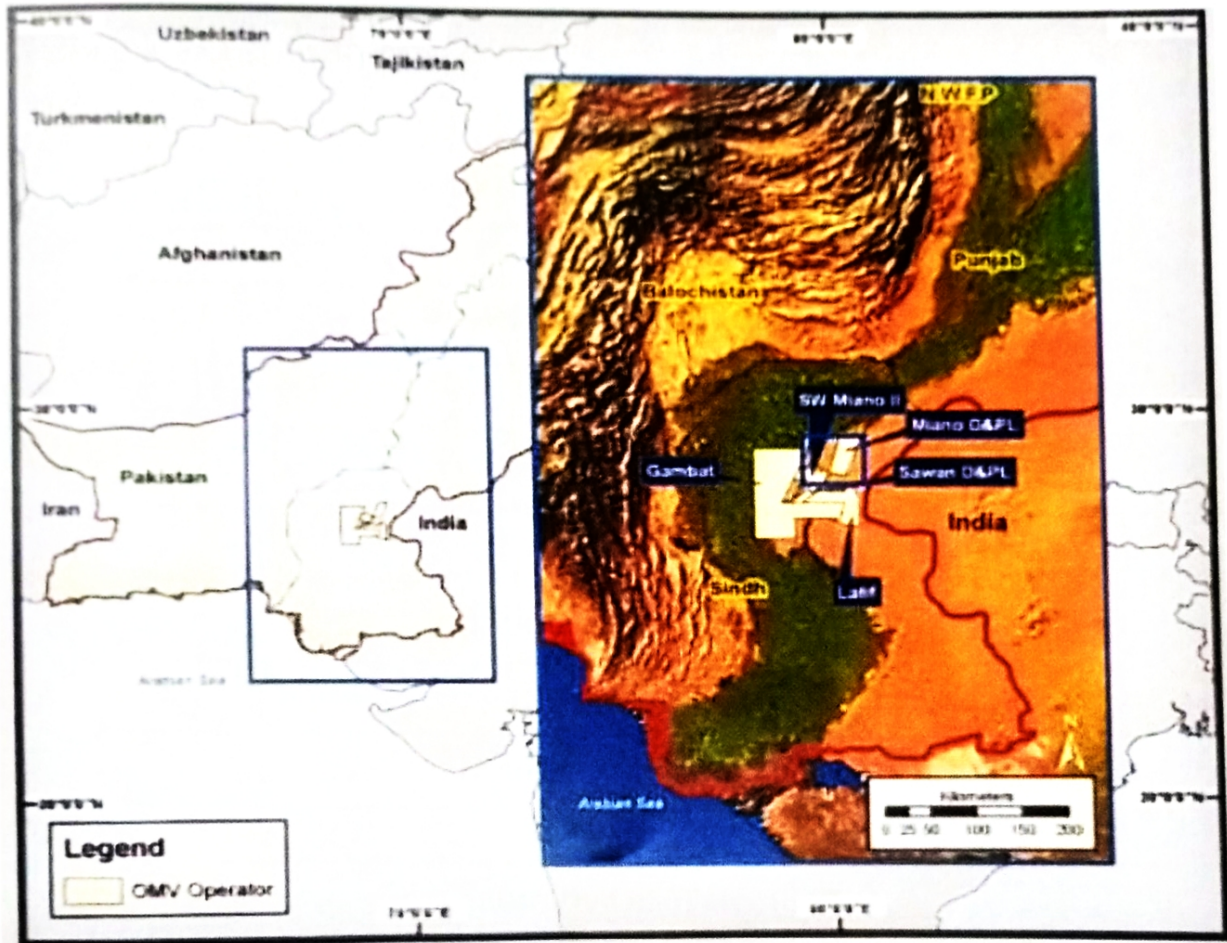


Figure 1.1. Location map of study well (Arc GIS 10.5)

1.3 Objectives

- To perform the petrophysical examination of Miano-09 well.
- To characterize the hydrocarbon capability of the reservoir of Miano-09 well.

1.4 Methodology

The methodology used to complete this research is shown in figure 1.2.

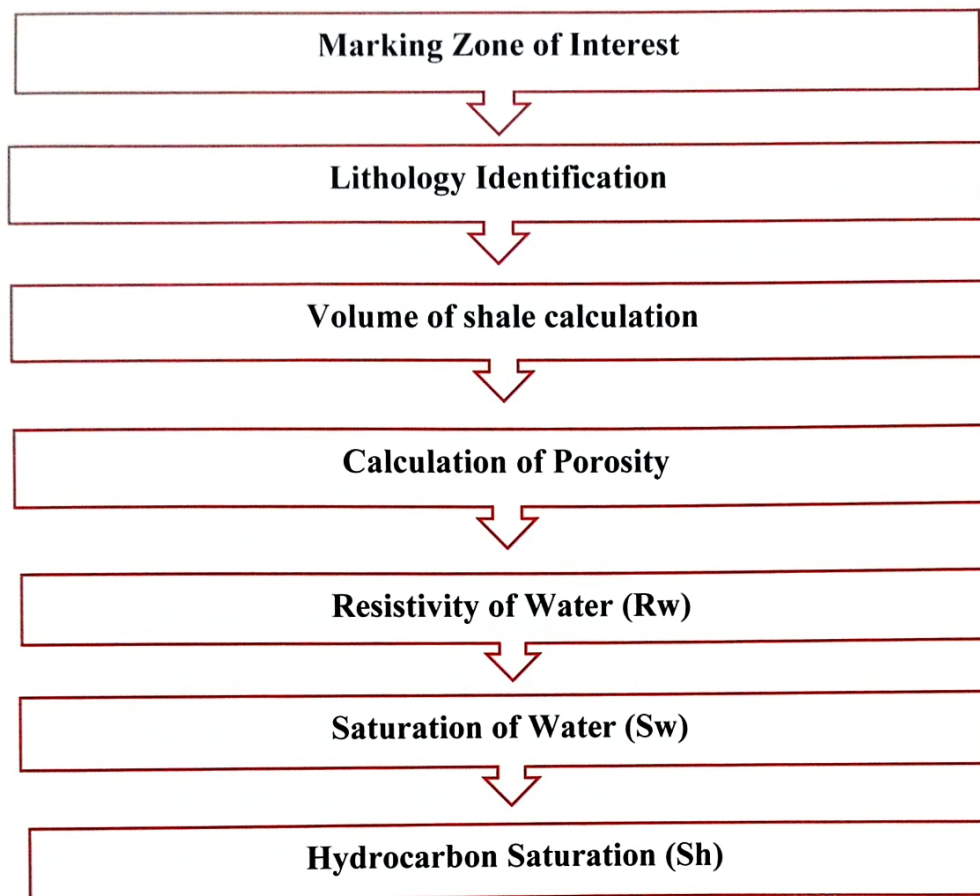


Figure 1.2. Flow chart displaying methodology adopted in the present study

CHAPTER 2

GEOLOGY AND TECTONICS

2.1. Regional tectonic setting of Pakistan

Pakistan is situated on the edge of the active platform, and is made up of two styles of boundaries of the Indian Eurasian and Arabian plates. The key point is that the Arab plate (oceanic plate) was subducted from the southwest part of Pakistan and that the Chagai volcanic arc was formed. The collision was triggered between the continent and the continent including the Indian and Eurasian plate collisions, resulting in Himalayan formation. In the western part of Pakistan the other plate frontier is the transforming plate boundary, which means that the Indian plate moves into the Afghan block which results in a fault shown in figure 2.1.

The portion known as the Indian plate is thought to be the Tethys Ocean in the Late Paleozoic Period, which was closed because of the Indian plate's northward collision. Permian sedimentation before the Cretaceous times filled the area that covered the Tethys Ocean. In Jurassic times, along with the African plate, Australian plate, and Antarctica, the Indian plate was isolated from the Gondwana floor. For the next 50 million, the Indian plate kept travelling northward and accelerating at a slow pace and turning northward until the Indian plate collided with the Eurasian plate. (Kazmi and Jan, 1997)

The pre-Owen fracture zone and the mid-Indian ocean ridge managed to displace the plate. The shift of the Indian plate towards the north is triggered by the subduction of the Intra-Ocean Collision, neo-Tethys closing and volcanic arches formation. The Indian plate and the present island arches were converted into the Kohistan Island and Ladakh Island, which are fit in between Indian and Eurasian plate.

The Indian plate shifted northward toward the Eurasian plate, contributing to the sedimentation and deposition of the Upper Indus Basin formation. Due to the movement of the Indian plate in the northern part of the Indian plate, faults were produced and the opposite Eurasian plate resisted, but the Indian plate used the force. The force exerted by the Indian plate was less than the resisting plate, which resulted in the subduction of the Indian plate under the Eurasian plate, resulting in the formation

of huge Himalayas due to the thrusting of this continent-continent collision. (Kazmi and Jan , 1997)

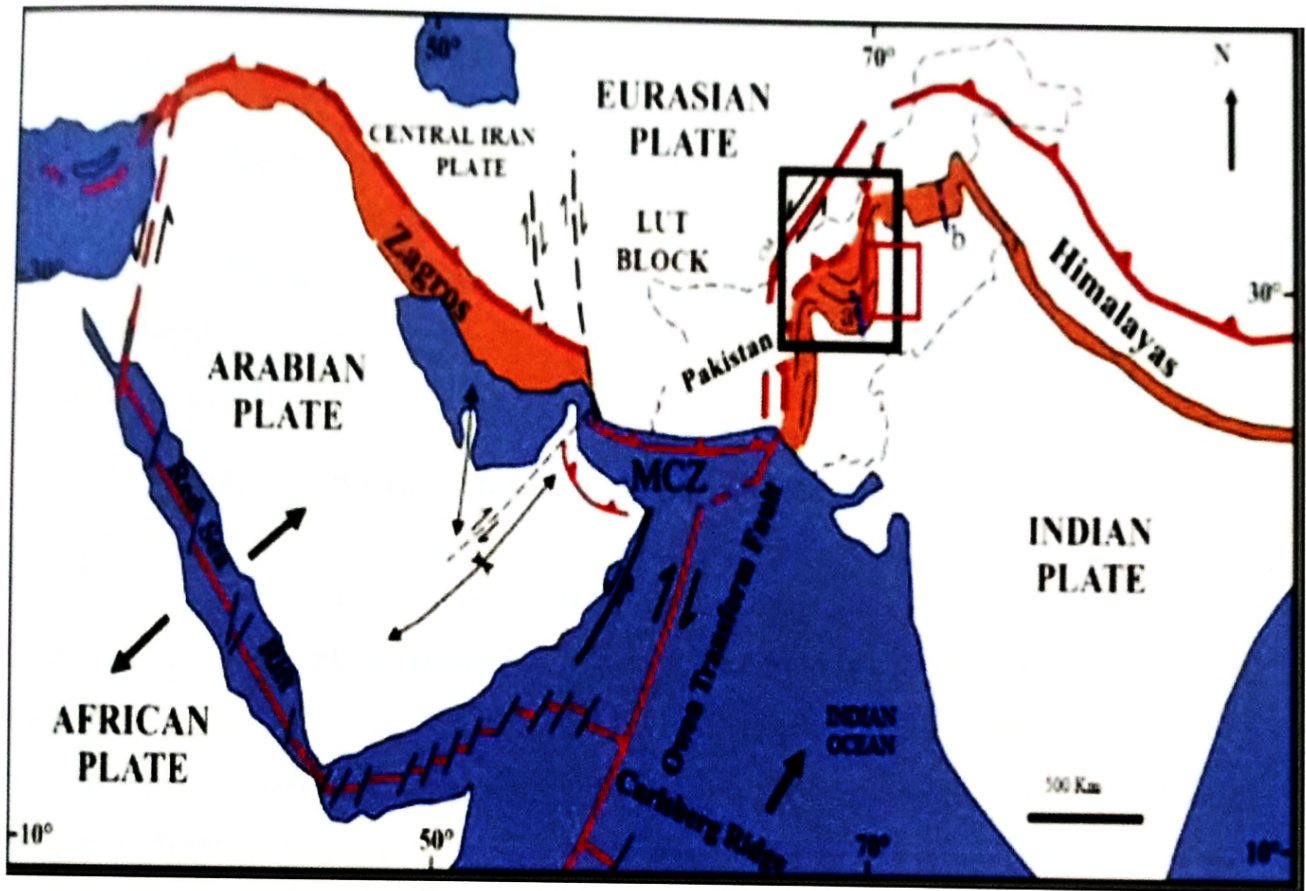


Figure.2.1.Regional tectonic setting of Pakistan (Jadoon, 2019)

The thrusting mechanism contributes to the formation of major faults i.e. MBT, MKT, MMT and SRT. One of the systems is the axial belt that divides the geosynclines and results in the formation of two reservoirs in Pakistan. Pre-collision forces and syn-collision result in the forming of structures. The belt formed the western edge of the Indian shield and separates the Indus Basin to the east and the Baluchistan Basin to the west and the tectonostratigraphic basins to the north.

The Indus basin is Pakistan's main basin and there are a number of studies about this basin. It is situated along its axis to the East of Pakistan and extend 'North East-South West' to over 1600 km². The Upper Indus Basin is about 50,000 km², while an area of 250,000 km² is occupied by the Lower Indus Basin. This Basin is separated by the Jacobabad Highs into the northern and southern Indus Basin. The upper Indus is retained in between by the (SRT) and (MBT). In the Upper Indus Basins, the two largest

reservoirs are separated. Potwar Sub-basin and Kohat Sub-basin. Kohat and Potwar sub-basin are separated by the Indus river. On the eastern and the west side of the Indus River are Kohat and Powder Sub Basins. The Indus Basin is characterised by syntax and irregular ridges, both trend NW.

2.2. Geological setting

The geological setting of the Miano area for its present position was briefly described in relation to the historical perspective of regional structure and sedimentation.

2.2.1. Basin architect of Miano and adjoining areas

The present Miano physiography and surrounding gas fields are abandoned due to the abundance of sand dunes. The field is 0 to 100 metres higher than the normal level of the sea. The geological progress of the region was dominated by a late rifting of Triassic deposits, the Pannu Aqil Graben was bordered by Jacobabad-Khairpur Horst to the north and Kandkot-Mari Horst to the south. The graben was known as Pannu Aqil Graben. The configuration of these geological characteristics is known as the Sukkur rift sub-basin, a revived rift system, in literature. The area obtained sediment during the intervening geological period. These horse-graben characteristics are related to the normal rooted basement faults, although intensive faulting occurred during the Mesozoic period, which led to the initiation of the Mari-kandkot and Jacobabad-Khairpur highs in the basement. During the Cretaceous era, these peaks were swelled and resumed to affect the depositional pattern during the Paleogene and Neogene eras. Subsequently, an oblique collision between the Indian and Afghan blocs resulted in a transgression regime affecting the region with a separate compression/strike-slip portion shown in figure 2.2.

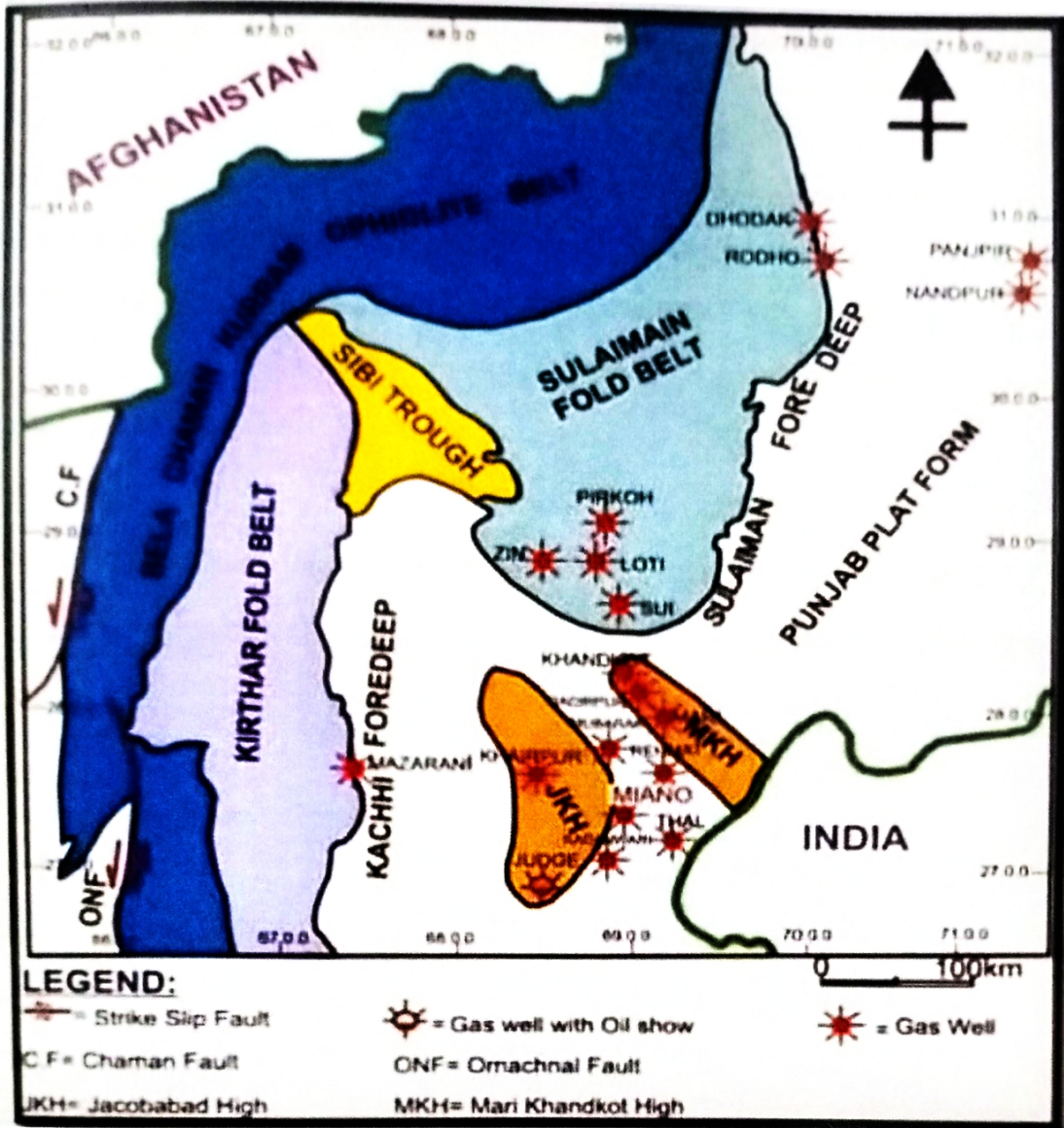


Figure.2.2. Tectonic map of study area (Bregar et al, 1997)

Chiltan claystone is the deepest penetrated sedimentary rock in the Middle Jurassic. The chiltan claystone was heavily damaged by the drowning dispute over the shutdown of the carbonate plant and a massively clastic sedimentation phase of sembar formation which led to a range of clinoforms with a source region to the East (mainly sand dominated). The top-of-the-grain layer is called Goru deposition, divisible in the lower Goru (sand, shallow alternating faces) and the upper Goru (shale, clay, marl and limestone facies). In the transgressive phase the lateral deposit has a number of marine depths. The early deposit for the low goru cretaceous over 15Ma was split into 4 subdivisions A, B, C and D intervals. The Goru A, B and C sands are built in this location as reservoir soil. The field of Miano is formed from the B sands. The upper Goru, composed of contrasting silt, shale, etc. Another raising of the sea level resulted

a further dip of the basin is eventually induced by the deposition of extensive pelagic mudstone facies such as Parh claystone. Some sections of the top formation of Parh have characterised the removal of the seal point, erosion and uplift at a regional level. An all-round transgression in paleocene resulted in the deposition of the ranikot consisting of a shale, siltstone, sandstone, etc. Historically the Ranikot formation has not been created as a reservoir rock, but it possibly has some variety.

2.3. Nomenclature of lower goru sands

The nomenclature of lower goru sands is shown in figure 2.3.

AGE	Fm.	OGDCL		UTP		LASMO	OMV	
CRETACEOUS	LOWER GORU	UPPER SANDS	"A" SAND	LAYER-1	UPPER SANDS	"A" SAND	SHALE OUT IN NORTH	SHALE OUT
			TURK SHALE	LAYER-2		TURK SHALE		
			"B" SAND	LAYER-3		"B" SAND		
			BADIN SHALE	LAYER-4		BADI SHALE		
			"C" SAND	LAYER-4		"C" SAND		
			JHOL SHALE			JHOL SHALE		
			"D" SAND	"D" SAND				
		UPPER SHALE	UPPER SHALE	"H" SAND (WITHIN UPPER SHALE)	NO SIGNIFICANT SAND BODY			
		MIDDLE SAND	MIDDLE SAND	"G" SAND	"D" SAND			
		LOWER SHALE	LOWER SHALE	"F" SAND (WITHIN LOWER SHALE)	"C" SAND			
		BASAL SAND	BASAL SAND	"E" SAND	"B" SAND WITH IN SHALE			
		TALMAR SHALE	TALMAR SHALE	"D" SAND "C" SAND				
MASSIVE SAND	LOWER BASAL SAND	"A" SAND	"A" SAND					
SEMBER	SEMBER	SEMBER	SEMBER					

Figure.2.3.Nomenclature of lower goru sands (Courtesy of ODGCL).

2.4. Generalized stratigraphy of Lower Indus basin

The Central Indus Basin is situated north of the Lower Indus Basin, north of the Suleiman Fold Belt and west of the Kirthar Fold Belt. The main tectonic mechanisms that have dominated the deposits and sediment delivery of the Lower Indus Basin are the rift of the Gondwanaland Indian Plate, which may have caused elevation

and eastward tilting at the beginning of the Cretaceous. With fold-thrust systems overlaid with sinistral flower structures, the Himalayan collision produced a sinistral transgression to the west of the Lower Indus Basin. (Shah et al., 1977 and 1980)

Infra-Cambrian to Clastic and Carbonate underlies this tectonic province. It stayed a passive margin until the late Cretan Sea, then it was part of the complicated suture of the Indian Plate and the Afghan Block. The stratigraphic sequence ranges in East-West direction. In the southeast corner of the basin there is revealed the Precambrian cellar. The thickness of the sediment rises to the west. At base Permian and base tertiary there are significant differences. The Tertiary associates closely in the eastern part of the basin with the Jurassic series as shown in figure 2.4.

2.4.1. Siwalik Member

In the northern Lesser Himalayas and south Indo-Gangetic Plains, the Siwalik Group is restricted. In total, the stratigraphical sequence reflects the upwards coarsening of the Himalaya, while any fluvial succession shows the upward finishing succession (e.g. mudstone, sandstone and conglomerate).

2.4.2. Kirthar formation

"Kirthar" name was used by Blanford (1876) after Kirthar Range to describe Eocene strata in Western Sindh between his 'Ranikot Group' and 'Nari.' Noeting later (1903) the lower part was divided by "Laki series" keeping for the upper part the word "Kirthar". Just. Here, as the Kirthar Formation, this top portion is formalised and equals the Spintangi Oldham's calendar (1890), also contains " of Oldham (1890). This formation also includes " and " with " Part of the Hunting Survey Company and member of "Gorag Member" of the Corporation (1961). Shah (1999) devised Kirthar as mainly calcareous with a certain shale, marl. The claystone is white, light-gray, crème, and grey, dark, or chalky. The shades of the milk. It is moderate to large, nodular in places and often contains algal and Structures of coral. The shale is olive, yellow orange, grey, limy, earthy. But in in the upper half of the unit is only huge in some parts of the province of Kirtar Hunting Survey Corporation's claystone ("Gorag member") (1961).

2.4.3. Drazinda Formation

Drazinda Formation as dark brown to grey Subordinate marl interbeds of fossiliferous clay. Increase up section with marl intercourse. The top Part is gypsizable as well. In the center there are fossil-brownish calcareous interbeds. The segment. A greenish-gray limestone unit about the thickness of 10 meters in the Gomal Pass region the middle part appears. The formation of Drazinda takes place in the Bugti Hills as a recognized unit Sulaiman Range's foothills. This formation winds up in the Spin Ghora Range in South Waziistan along with the Pirkoh and the Domanda Formations. (Shah et al., 1977 and 1980)

2.4.4. Pirkoh member

Hemphill and the "Pirkoh limestone member". The later author's "White marl band" was also used in Kidwai (1973) for the coeval unit of "Pirkoh limestone and Marl Member" of Eames (1952). Pirkoh formation consists of light grey to white calcareous calcareous, brown buffed, ungrained, often thin, and regularly lined with clay. The formation typically consists of subordinate sot, shay calcareous and dark grey clay. The Pirkoh Formation forms continuous ridges in the foothills of the range of Sulaiman and the region of Bugti. The diameter ranges from 10 to 175 m. The formation is 135 meters thick in the area of Pirkoh, 40 meters in the area of Zin, 35 meters in the south and the north of Waziristan near the Shinki post.

2.4.5. Sirki member

The era of Sirki Member belongs to Eocene. The interval between 880m and 930m is deep. This member has a total thickness of 50 m. The lower touch is also comfortable with Habib Rahi Member. The deposition environment is also poor in the marine environment. Sirki Member's top contact consisted of the lithological transition between claystone and calcareous. Claystone has a lightly calcareous, soft to firm dark bluish green colour. Limestone displays a moderately hard light, yellowish grey colour with signs to forams. (Shah et al., 1977 and 1980)

2.4.6. Habib Rahi formation

Habib Rahi formation has a brown grey and rough calcareously buffed this white weathering. It is obscure, small, dominantly clayish, except in a few places it is marble-like. The upper part of the training which contained main with abundant *Assilina* restricts thin beds present in the reservoir. (Shah, 2009)

2.4.7. Ghazij member

The word 'Ghazij' for shale beds between Oldham (1890) Spintangi and Dungan Formation in southeastern Hamai Spintangi (Ghazi Formation after Williams 1959). It was officialised by the Stratigraphic Committee of Pakistan, which was a synonym of all other names such as "Shale with Alabaster, trash calcareous. Eames's (1952) and Ghazij Shales Upper Rakhi Gaj Shales and Zindapir Limestone, " Team Ghazij, to consists of subordinate shale. The local commercial value becomes abundant with claystone, sandstone, claystone, conglomerates and even alabaster and coal. The group includes pale greenish or brown shale, white or pale grey calcareous. In some areas, sandstone is a subordinate portion but strongly calcareous and sandy calcareous. (Shah et al., 1977 and 1980)

2.4.8. Laki Formation

The Laki formation is mainly formed in the Southern Part of the Province of Kirthar and the Sulaiman Province, near the Mari-Bugti Hills. It is around 240 m in BaraNai and in the MaiNai style area, but at Tatti (province of Kirthar) and Sui, where the surface is found and reaches the thickness of 468 m, reaches a thickness of more than six hundred m. The Laki Formation is underscored by the Ranikot Group and the base of the Member Sohnari is the touch. In most areas of the Kirthar province the highest interaction with the Kirthar Formation is compliant. The formation of the Ghazij Group is superimposed on the southern parts of the Kirthar province and its entire creation in the Mari-Bugti hills. Nai Formation and Siwalik Group unmistakably overshadow it in many localities in Laki Range.

2.4.9. Sui main limestone

The primary limestone age of Sui is the Lower Eocene. Atmospheric deposition conditions are known as superficial marine. Calvary with subordinate shale beds dominates the Sui Main Limestone. The limestone of white, white-grey, white light, white dirty, medium to rough, thick, micro-crystalline to crystalline, micrite, bio-clastical, broken at points. Limestone(wackstone). Carbonate/argillaceous material fills cracks, sometimes blurry, molten, pyritic, mega and microfossils are common. (Shah et al., 1977 and 1980)

2.4.10. Ranikot formation

The name 'Ranikot Community' was named for the first time in Blanford (1876). Sind, in the northern part of the Laki range, after Ranikot Fortress. He used the name to designate strata that lie between his "volcanic" and his "Kirthar or Lower Nummulitic Group" Also named Blanford "Intra-Nummulitic" Ranikot party. The Ranikoth group was redefined in 1879 and he was removed from "Cardita beaumonti beds" and the "Trap group" ("Cardita beaumonti Beds"), called later (1879) as part of his Ranikoth group. The original description of the group by Blanford is preserved and this group is regarded as representing strata known as "Betrap Group" and "Ranikot Group." Cardita Beaumonti Beds The redefined "Ranikot Group" of Blanford was subdivided into Vredenburg's "Lower Ranikot (sandstone)" and the "Upper Ranikot (limestone)" (1909a). The present report includes this subdivision.

2.4.11. Parh Limestone

Blanford's (1879) word "Parh" was used for the Parh rocks. Later, in his Cretaceous succession, Vredenburg (1909) applied the name to a prominent white limestone. The Goru and Mughal Kot formations were redeveloped by Williams (1959). The region of type is located on the top of the Gaj River in the Parh Range. The lithological distinct unit is the Parh Limestone as defined by Fatmi (1977). It has a hard, light grey, white, creamy green olive oil, slim to medium-sized, porcelain graphic and argillaceous sometimes flat to slabby calcareous. Intercalation. It is distinguished by its porcelain appearance and its conchoid fracture in other calcareous

units. In the lower portion, close contact with the Goru formation a stubborn maroon-colored calcium bed is formed.

2.4.12. Goru formation

The Goru formation is made up of calcareous intercouched, shale and siltstone. The calcareous is unknown, small, medium to light grey and grey olive. The silt and shale are interlinked in grey, and maroon locally. The shale differs widely and the dominant rock type is positioned. The lower and upper sections of the formation dominate the calcareous. In both the Kirthar and the Goru formation are widespread provinces of Sulaiman. In the type area, the thickness is 536 m, but near Quetta the width decreases to 60 m. More than 100 m was reported in the subsurface. (Shah et al., 1977 and 1980)

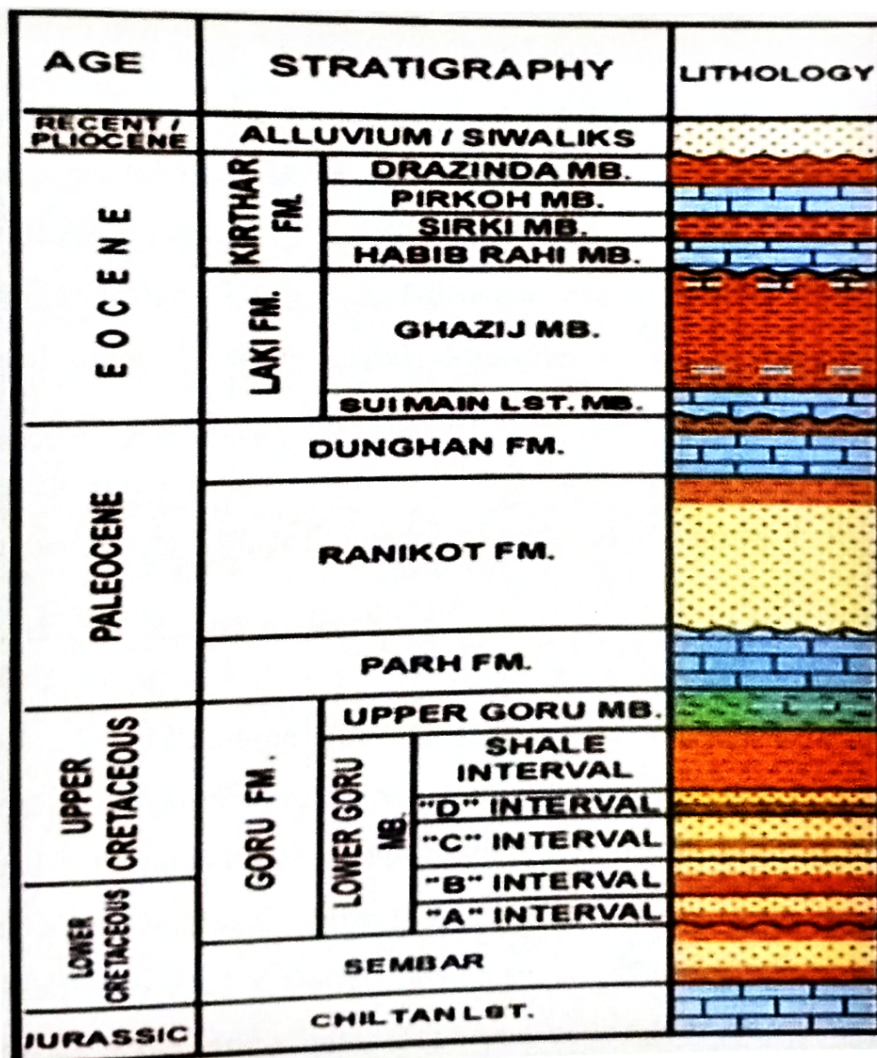


Figure.2.4.Stratigraphy of lower indus basin (Wandrey et al., 2004)

2.5. Petroleum System of lower Indus basin

For the lower Indus Basin, the Basin-wise performance rate was the highest (due to strings of rapid succession finds in relatively small tilted fault Blocks in the pool of lower Goru). Throughout the 1980s, a range of oil/gas/condensate discoveries were made in the Lower Goru Formation. Exploration activities were further developed in the 1990s, when several important gas finds were made in the Late Cretaceous clastic (e.g. the findings of Bhit & Zamzama). (Kadri, I.B, 1995)

2.5.1. Source Rock

Sembar has been identified as the main source rock for most of the Greater Indus Basin, and there are other known and possible source rocks. Rock units containing proven or possible source rocks include the Salt Range Formation 'Eocambrian' shales, Permian Dandot and Tredian Formations, Triassic Wulgai Formation, Jurassic Datta Formation, Paleocene Patala Formation, Eocene Ghazij Formation, and lower Miocene shales. Miocene rocks are thought to be good hydrocarbon deposits in the offshore regions of the Indus Geological Province, with Sembar being added to the shelf area. The Ghazij Formation sandstones are coherently overlaid with the Eocene Kirthar Formation's interlaced limestones and shales.

2.5.2. Reservoir Rock

Limestone from the Habib Rahi and Pirkoh members of the Kirthar Formation are possible reservoirs in the Eocene. The primary reservoir in the Dhodak oil and gas field is Ranikot sandstone. Within the Mughal Kot Formation, the Pab sandstone along with sand horizons is the most potential reservoir in about the area. At the Rodho gas field of Dewan Petroleum, Sember and Lower Goru sandstone of the Cretaceous period and Chiltan limestone of the Jurassic age have measured commercial quantities of hydrocarbons. Deltaic and shallow coastal sandstones and Lumshiwai deposits in the middle Indus Basin and the calcareous stones in the Eocene of Ghazij and equivalent stratigraphy units comprise the main reservoirs of the lower Indus Basin in the lower Indus formation. There can be lakes up to 400 m deep. Porosity

of sandstone is as high as 30%, but typically ranges between 12 and 16%, and porosity of claystone varies between 9 and 16%. These reservoirs have a permeability between 1 and 2,000 millidarcies (md). In the Eocene Sui Main Limestone Member, 625 m thick, were the highest reserves.

2.5.3. Seal Rock

The identified seals in the system consist of shales, in particular intra-formational shale for the Lower Cretaceous reservoirs, which are interspersed with and overlying the reservoirs. Thin shale beds with varying thickness are effective seals in processing fields. The impermeable seals above the truncation traps, faults and changes in the dip facies provide additional seals that can be successful.

2.5.4. Traps

The identified seals in the system consist of shales, in particular intra-formational shale for the Lower Cretaceous reservoirs, which are interspersed with and overlying the reservoirs. Thin shale beds with varying thickness are effective seals in processing fields. The impermeable seals above the truncation traps, faults and changes in the dip facies provide additional seals that can be successful.

2.6. Bore-hole stratigraphy

The encountered formation in borehole during the drilling shown in table 2.1.

Table 2.1. Bore-hole stratigraphy of Miano-09 well.

Well Name	Well Bore	Formation	Formation Age	Formation Tops (m)	Thickness (m)
Miano-09	Miano-09	Siwaliks	Pliocene	0	497
Miano-09	Miano-09	Kirthar Fm	Eocene	497	0
Miano-09	Miano-09	Drazinda Member	Eocene	497	75
Miano-09	Miano-09	Pirkoh Member	Eocene	572	103
Miano-09	Miano-09	Sirki Member	Eocene	675	67
Miano-09	Miano-09	Habib Rahi Member	Eocene	742	129
Miano-09	Miano-09	Ghazij Member	Eocene	871	0
Miano-09	Miano-09	Laki	Eocene	871	641
Miano-09	Miano-09	Sui Main Limestone Member	Eocene	1512	185
Miano-09	Miano-09	Ranikot Formation	Pleocene	1697	163
Miano-09	Miano-09	Parh Formation	Early Cretaceous	1860	70
Miano-09	Miano-09	Upper Goru	Early Cretaceous	1930	0
Miano-09	Miano-09	Goru	Early Cretaceous	1930	331
Miano-09	Miano-09	Shale Unit	Early Cretaceous	2261	1070
Miano-09	Miano-09	Lower Goru	Early Cretaceous	3331	-

2.7. Petroleum play

In Miano-09 well sembar formation is acting as a source rock. Sands of B-interval are acting as reservoir rock while the shale unit of Goru Formation is acting as cap rock. The petroleum play of Miano-09 well is shown in table 2.2.

Table 2.2. Petroleum play of Miano-09 well.

Petroleum Play	Formation	Age
Seal	Intraformational Shale of Lower Goru	Cretaceous
Reservoir Rock	Lower Goru	Cretaceous
Source Rock	Sembar formation	Cretaceous

CHAPTER 3

PETROPHYSICAL ANALYSIS

3.1. Introduction

The word Petro-physics is derived from two Greek terms i.e. Petro which means 'Rock' and Physics which means 'nature'. Study of chemical and physical rock properties and their relation with fluid involves the petrophysical analysis. Data of Petro-physical analysis can be achieved by log and laboratory data. By taking and analyzing well log measurements by instruments that are placed in the borehole or taking core samples, Petro physicists test source rock or reservoir.

By calculating water saturation and then hydrocarbon saturation, the key goal is to quantify or measure the hydrocarbon potential in the reservoir. Saturation of hydrocarbons means that how much pores in the rock are filled or saturated with the hydrocarbons.

3.2. Methodology

For the successful interpretation of the Miano-09 well, our priority was to check the quality of the logs means taking the readings at every depth. Following are the different petrophysical parameters which are calculated;

1. Volume Of Shale (Vshale)
2. Volume Of Clean (Vclean)
3. Effective Porosity (EPI)
4. Resistivity Of Water (Rw)
5. Saturation Of Water (Sw)
6. Saturation Of Hydrocarbon (Sh)

3.3. Log Trends of Miano-09 well

In the given log as shown in figure 3.1 Bit size, Gamma ray and Calliper log is shown in Track 1. The information that we can interpret with the help of Calliper log and Bit size is the bore hole geometry i.e. the bore hole is Gauged (Bit size=Calliper), Under Gauged (Calliper<Bit size) or Over Gauged (Calliper>Bit size).

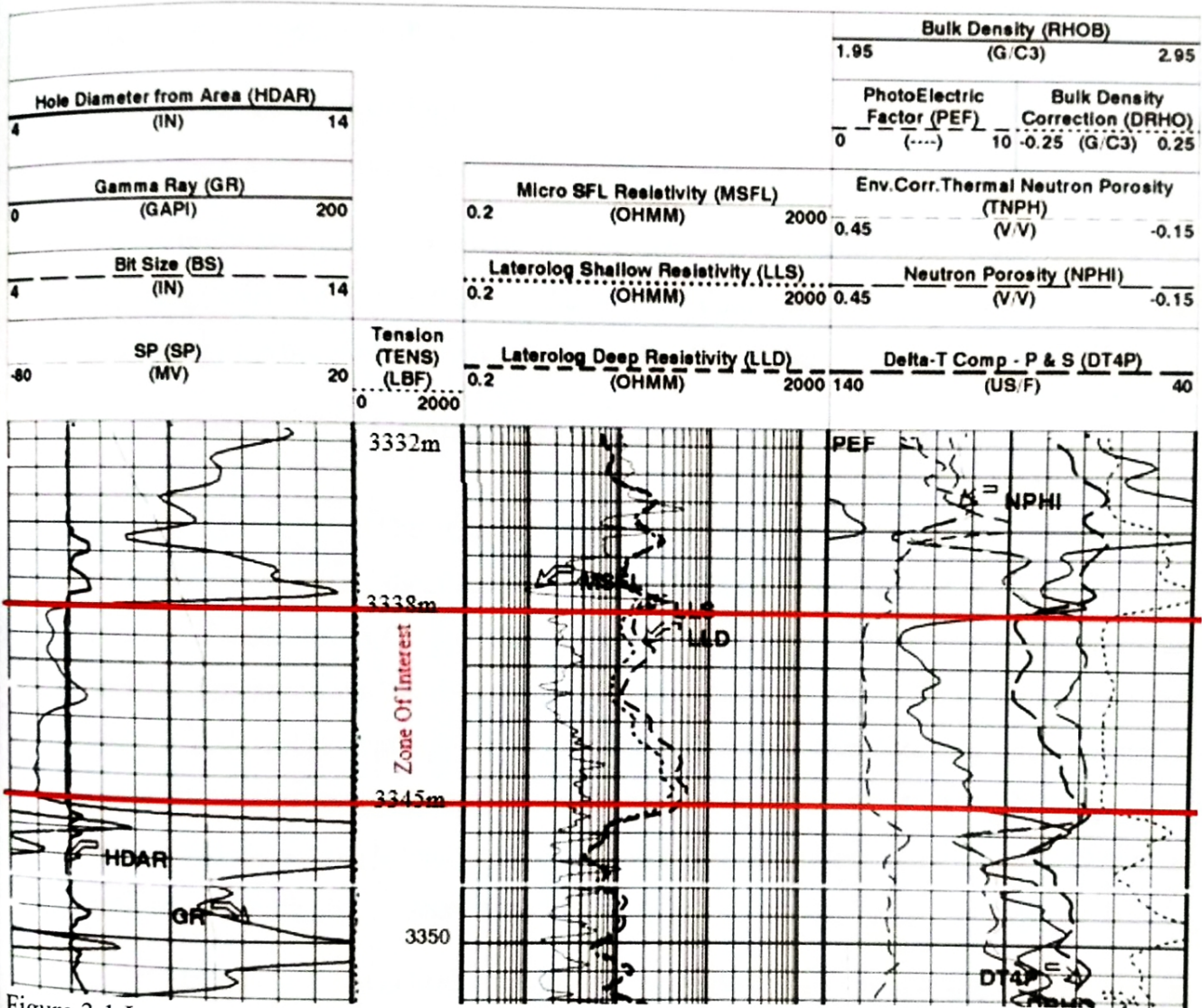


Figure.3.1. Log trend showing depth interval of the zone of interest(3338m-3345m)

3.4. Data used

3.4.1. Calliper Log

A calliper log is a well logging instrument that allows the size and shape of a borehole along its depth to be continuously measured. As it is removed from the bottom of the hole, using two or three articulated arms that press against the borehole surface, the calliper instrument measures the difference in borehole diameter. There are two types of calliper tool;

1. Two arm calliper tool.
2. Four arm calliper tool.

In the two arm instrument, the diameter of the borehole is measured. The two opposing pairs work together in the 4-arm (dual calliper) instrument to give the diameter of the borehole in two perpendicular directions.

3.4.2. Gamma Ray (GR) Log

The Gamma Ray (GR) instrument measures radioactivity naturally present from the formation. The unit of Gamma Ray log is API (American Petroleum Institute). A GR log allows to separate shales and clays from reservoir rocks, such as sandstone and carbonates, from non-reservoir rocks. Shales and clays are derived from rocks that appear to contain radioactive elements that exist naturally, especially potassium, uranium, and thorium. As a result, shales and clays are more radioactive than sand-stones and carbonates that are clean. Almost no radiation is emitted by quartz and calcium carbonate.

If radioactivity is high, the GR curve would be high, indicating the presence of dirty lithology, such as clay or shale. If the GR curve is low, it suggests the presence of clean lithology, regarded as a reservoir, such as limestone or sandstone. The key aim of this instrument is, thus, to mark the reservoir by telling the quantity of:

- Radioactive elements
- Radioactivity energy

3.4.3. Spontaneous potential (SP) Log

In the absence of any artificially applied current, the spontaneous potential log (SP) calculates the normal or spontaneous potential difference (sometimes called self-potential) that occurs between the borehole and the surface. It is a calculation of the difference in voltage between a movable electrode in the wellbore and a surface fixed electrode. This electrical potential is produced primarily by the exchange of fluids in the mud system and in the creation of various salinities. Permeable rock within the wellbore is invaded during the process of exploration by drilling mud filtrate. Negatively charged chlorine ions from the formation water allow the SP curve to deflect to the left from an arbitrary baseline formed over impermeable shale formations if the filtrate is less saline than the formation fluids. A variety of variables, including permeability, porosity, water salinity formation and mud filtrate characteristics, affect the extent of the deflection.

There are four principal uses for the SP log:

- Identification of beds with permeability.
- R_w determination.
- Indication of the shaliness of a formation.
- Correlation.

3.4.4. Resistivity log

Resistivity instruments calculate the development at various investigation depths. The resulting log exhibits curves of shallow, medium and deep reading. The shallow curve indicates the resistivity of the flushed zone around the borehole, mapping the lowest inquiry radius. The medium curves suggest the invaded zone's resistivity. The deepest curves represent the uninvaded zone's resistivity, which is assumed to be the true resistivity, but the presence of mud filtrate can affect even the deepest reading curves.

There are three types of resistivity logs i.e.

1. Micro-spherically Focused Log (MSFL)
2. Lateral Log Shallow (LLS)
3. Lateral Log Deep (LLD)

Since water is low-resistive and hydrocarbons are high-resistive, the resistivity log will easily highlight hydrocarbons. The distinction between the LLS and LLD curves suggests the availability of fluid for formation. The three resistivity instruments listed above are ideally equipped to test correct resistivity in formation by putting MSFL in the flushed region, LLS in the transition zone, and LLD in the true zone or uninvaded zone.

3.4.5. Bulk Density Log

Formation bulk density provides an essential porosity indicator. A formation's bulk density (RHOB or Pb) is dependent on the ratio of the mass of a measured interval to its volume. Porosity, in general, is inversely related to rock density. The Pb calculation is obtained from a formation's electron density. A logging tool that emits gamma rays into the formation receives this measurement. In a method known as Compton Scattering, the gamma rays clash with electrons in the formation, sending off energy and scattering. The number of such collisions in the formation is directly proportional to the number of electrons. Many of these dispersed gamma rays in low-density formations was able to penetrate the detector than in higher-density formations.

3.4.6. Neutron log

The neutron log is specifically sensitive to the number of atoms of hydrogen in a formation. Its primary use is in the calculation of a formation's porosity. The abundance of hydrogen atoms can be used to assess the fluid-filled porosity of a formation, since hydrogen is a significant constituent of both water and hydrocarbons, and because water and hydrocarbons accumulate in rock pores. Atoms of hydrogen have about the same mass as neutrons. Using a chemical source or an electrical neutron generator, neutron logging instruments emit neutrons. When these neutrons collide in a formation of hydrogen atoms, they lose full energy, slow down and gradually enter a state of very low energy or thermal energy. The rate of neutrons entering the thermal state is proportional to the concentration or index of hydrogen (HI). The HI, which is then transformed to neutron porosity, is calculated by Neutron porosity instruments.

There are two types of neutron tool which are as follows:

- I. Gamma-ray- Neutron tool (GNT)
- II. Compensated Neutron tool (CNT)

3.5. Zone Of interest

B interval sands of Lower Goru formation is only the zone of interest of 7m ranging from 3338m to 3345m as shown in (Fig. 3.1) and Table 3.1. This zone is marked on the basis of gauged bore hole condition, stable and low gamma ray value and separation between MSFL and LLD curve i.e. low MSFL and high LLD value.

Table 3.1. Zone of interest in Miano-09 well.

Formation	Formation Top (m)	Formation Base (m)	Zone Thickness (m)
Lower Goru	3338	3345	7

3.6. Petrophysical analysis of Miano-09 well

3.6.1. Calculating Volume of Shale (Vsh)

The quantitative calculation of dirt in the zone of interest is the amount of Volume of shale (Vsh). A gamma ray log is used to calculate it. High radioactive content represents increased gamma ray log value, shows dirt in lithology. On the other hand, decreasing gamma ray log value reflects clean lithology, indicating a lack or low radioactive material concentration.

Volume of shale is calculated by the following formula:

$$Vsh = \frac{GR_{log} - GR_{min}}{GR_{max} - GR_{min}}$$

Where;

Vsh= Volume of shale

GRmax= Maximum gamma-ray (Highest peak of a gamma-ray from a log)

GRmin= Minimum gamma-ray (lowest value of gamma-ray from a log)

GRlog= Value of gamma-ray at each specified depth

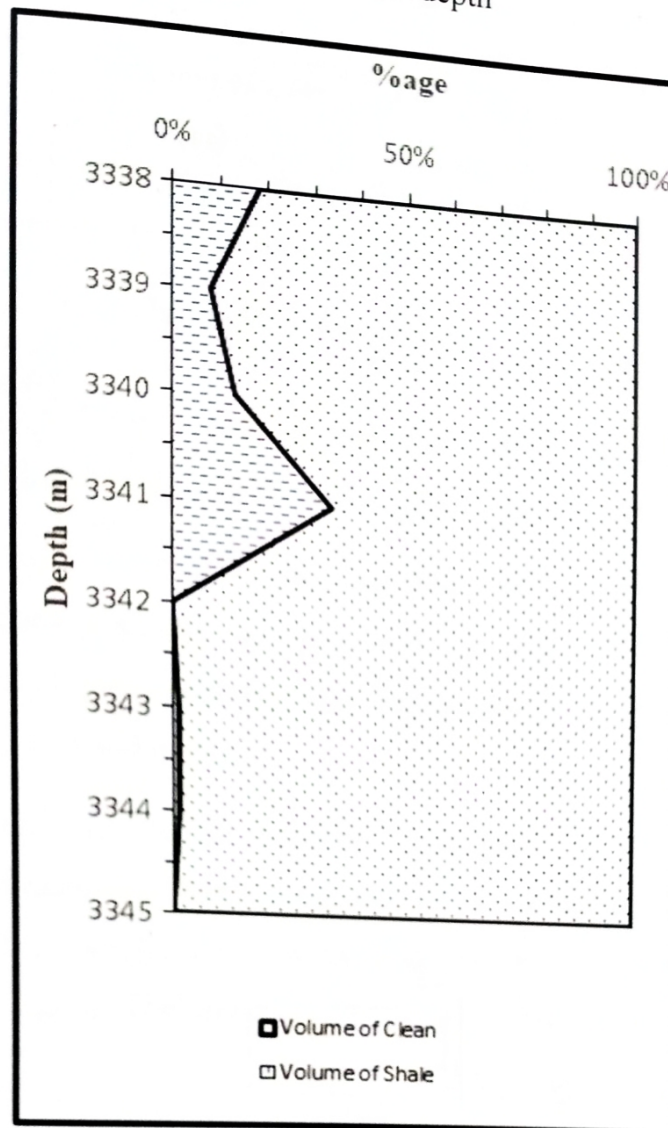


Figure.3.2. Cross plot showing the volume of shale and volume of clean against depth

In the zone of interest starting at depth 3338 m and ending at depth 3345 m, within the B interval sand, the figure 3.2 reflects a cross plot between the volume of shale and volume of clean. It is clear from the figure that within the zone of interest there is a certain shift in the amount of shale. At the beginning, the volume of shale is moderate and then it declines steadily at the end of the zone.

Table 3.2. The average volume of shale and the average volume of clean of the zone of interest.

Formation	Thickness of zone (m)	Avg. Volume of Shale (%)	Avg. Volume of Clean (%)
Lower Goru	7	9.43	90.56

3.6.2. Calculating Neutron porosity

Using a neutron log, the overall porosity of the zone is measured. Neutron log directly tells about the porosity in API unit.

Neutrons are slowed down and absorbed very rapidly and within a short distance in formations of a large number of hydrogen atoms. The slow neutron count rate or the detection of gamma rays is low in the instrument. Therefore, in high porosity rocks, the counting rate will be low.

The neutrons are slowed down and absorbed more slowly in formation containing a small number of hydrogen atoms, and travel farther into the rock before being absorbed. Therefore, the slow neutron count rate or the capture of gamma rays in the instrument is higher. The count levels would also be higher in rocks with low porosity.

Table 3.3. Average neutron porosity

Formation	Zone depth interval (m)	Avg. Neutron porosity (%)
Lower Goru	3338-3345	3.12

3.6.3. Calculating Density porosity (DPHI)

The density log measures the density of a formation's electrons. The logging system is a contact instrument from a source that emits gamma rays. Emitted gamma rays collide with electrons that form and diffuse. A detector, placed a fixed distance from the source of the tool, records the number of gamma rays returning. The number of returned gamma rays is a measure of the bulk density of the formation. Following formula is used to calculate the density porosity (DPHI):



$$\Phi = \frac{\rho_{ma} - \rho_b}{\rho_{ma} - \rho_f}$$

where:

- Φ = porosity
- ρ_{ma} = matrix density (2.71 for sandstone)
- ρ_b = formation bulk density (from log)
- ρ_f = density of the fluid saturating the rock immediately surrounding the borehole—usually mud filtrate (1.0 for freshwater and 1.1 for saltwater mud)

Table 3.4. Average density porosity

Formation	Depth interval (m)	Avg. Density porosity (%)
Lower Goru	3338-3345	23.62

3.6.4. Calculating Effective porosity (EPI)

Effective porosity is the volume or amount of pores available in a rock that are interconnected. Effective porosity is often lower than the total porosity (API). Effective porosity matters largely because it reflects how much fluid is going to pass. Relation between EPI, API and V_{shale} is shown in figure 3.3. If sonic porosity is not available, then the following equation is used to measure effective porosity:

$$\varphi_e = API * V_{clean}$$

Where;

φ_e = Effective porosity

API = average total porosity

V_{clean} = Volume of clean

Table 3.5. Average Effective porosity

Formation	Zone depth interval (m)	Avg. Effective porosity (%)
Lower Goru	3338-3345	12.02

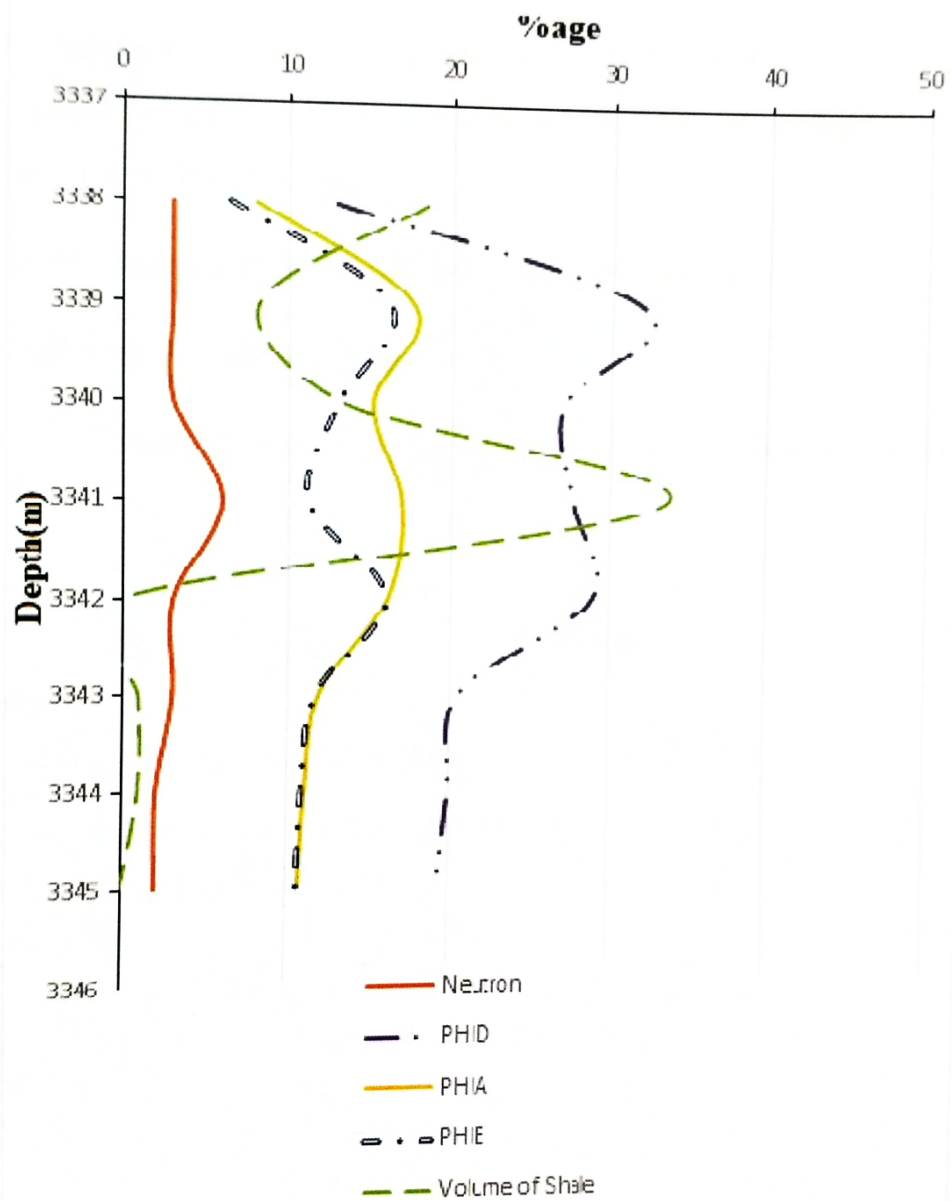


Figure.3.3. Relation between Vshale and porosities

3.6.5. Resistivity of water

It is the main and most sensitive method for the measurement of water saturation and hydrocarbon saturation is determined from water saturation. If the

water resistivity is high, it will cause high saturation of water and low saturation of hydrocarbons, and vice versa. Water resistivity is evaluated by three processes, which are as follows:

1. Method with SP
2. Method picket plot
3. Method with apparent resistivity (R_w)

The most accurate approach is the SP method, and Apparent R_w is the least accurate method for water resistivity calculation. So, the SP approach has been used here to determine water resistivity.

The SP method requires a total of seven following steps:

i. Geothermal gradient of well

Following is the formula for the calculation of Geothermal gradient;

$$G. G = \frac{B. H. T - S. T}{\text{Total Depth}}$$

Where

B.H.T (Bottom Hole Temperature) = 320°F

S.T (Surface Temperature) = 80°F

Total Depth = 3383m

$$\begin{aligned} G. G &= \frac{B. H. T - S. T}{\text{Total Depth}} \\ &= \frac{320^\circ\text{F} - 80^\circ\text{F}}{3383\text{m}} \\ G. G &= 0.0709^\circ\text{F/m} \end{aligned}$$

ii. Formation temperature

Following is the formula for the calculation of the formation temperature:

$$F. T = (G. G * \text{Formation Top}) + S. T$$

Where

Formation Top = 2261m

$$\begin{aligned} F.T &= (G.G * \text{Formation Top}) + S.T \\ &= (0.0709 * 2261) + 80 \end{aligned}$$

$$F.T = 240.30^{\circ}\text{F}$$

iii. Rmf at S.T (Surface Temperature) \longrightarrow Rmf at F.T (Formation Temperature)

Using Gen-9 chart

Rmf at Measured Temperature = 0.151ohm.m

0.151ohm.m \longrightarrow 0.052ohm.m

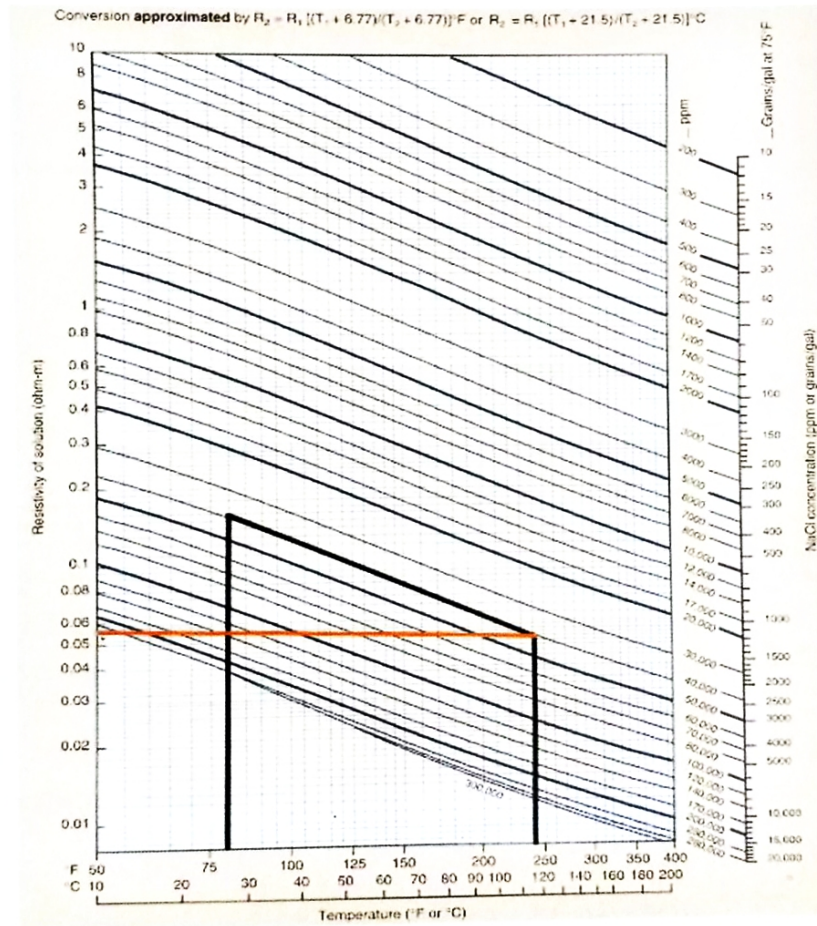


Figure.3.4. Conversion of RMF@S.T to RMF@F.T using Gen-9 chart

iv. Rmf \longrightarrow Rmfeq

As R_{mf} is less than 0.1 ohm.m so we will use SP-2 chart to derive the value of R_{mfeq} at formation temperature.

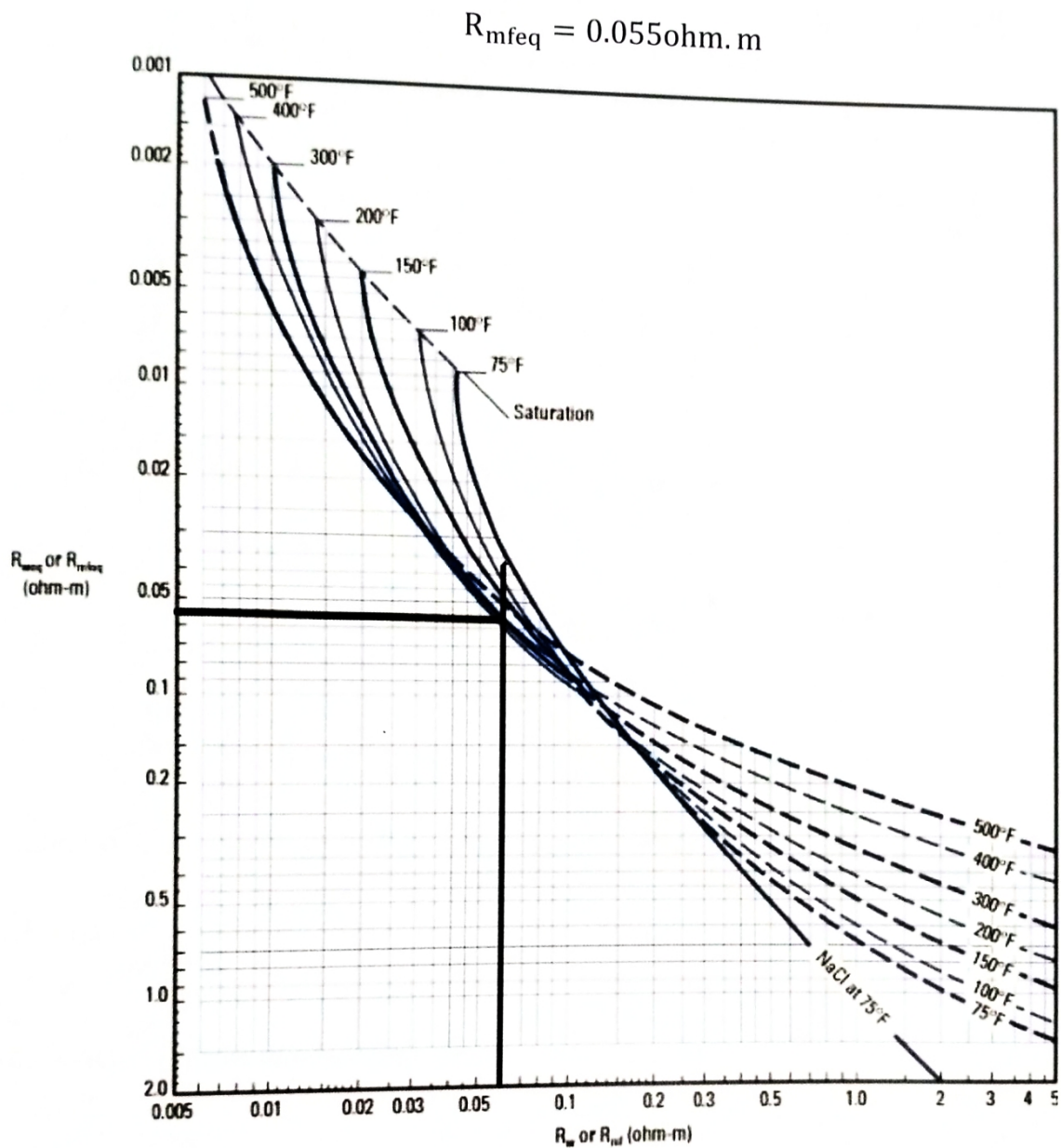


Figure.3.5. Conversion of R_{mf} to R_{mfeq} using SP-2 chart

v. Calculate SSP (Static Spontaneous Potential) using SP log.

$$SSP = +5MV$$

vi. SSP and R_{mfeq} \longrightarrow R_{weq}

Using SP-1 chart

+5MV & 0.055 \longrightarrow 0.04ohm.m

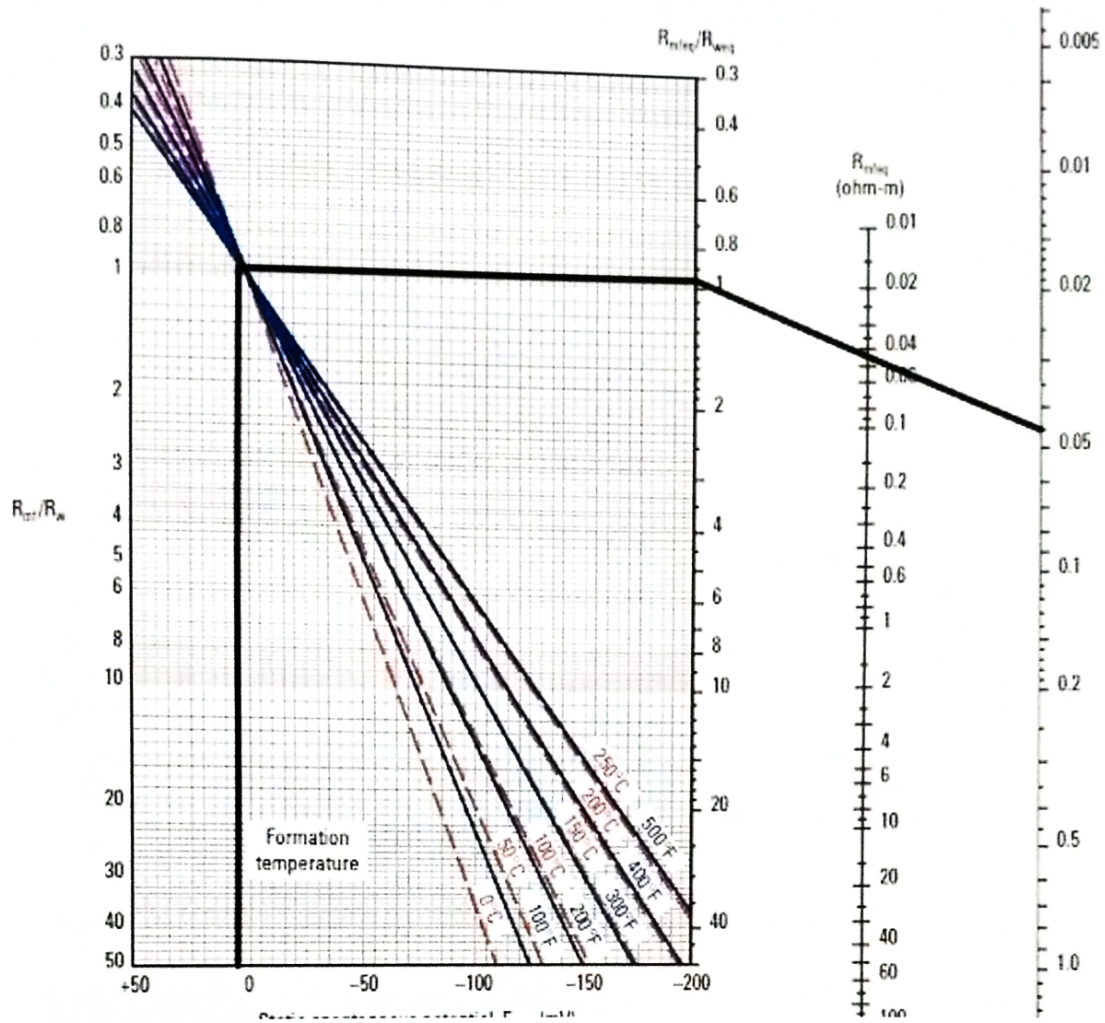


Figure.3.6. Conversion of SSP and Rmfeq to Rweq using SP-1 chart

vii. $R_{weq} \longrightarrow R_w$

Using SP-2 chart

$0.039 \longrightarrow 0.05 \text{ ohm.m}$

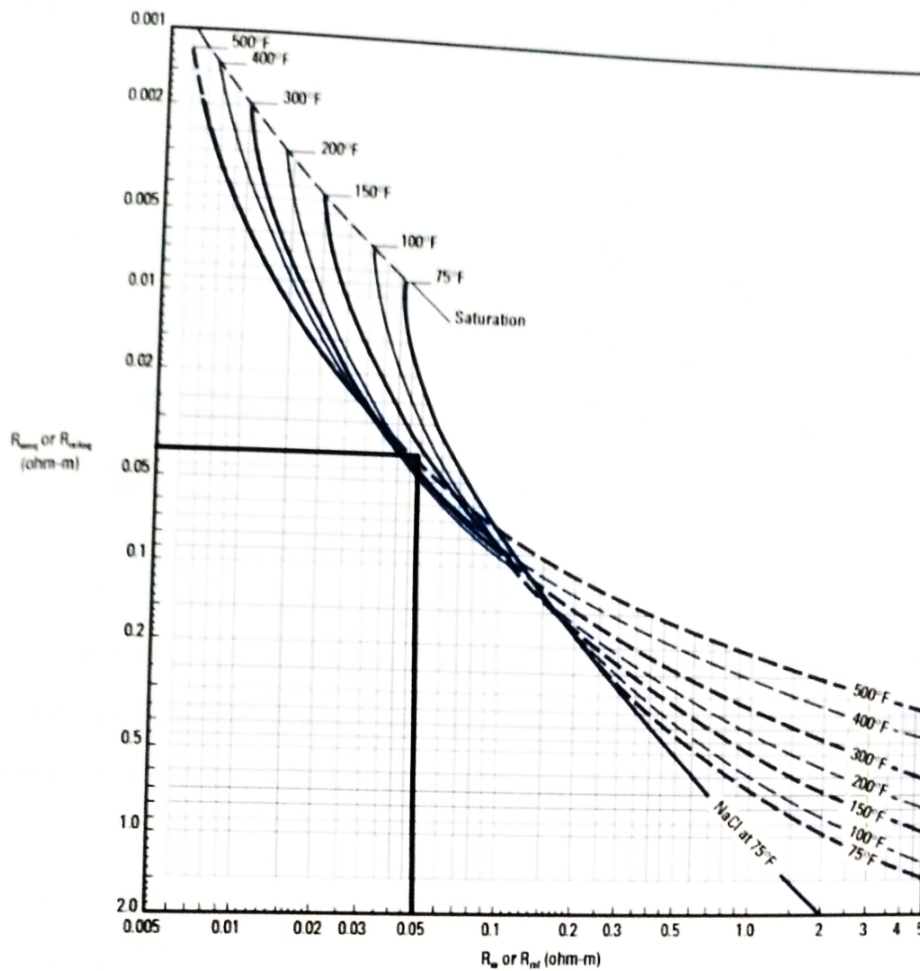


Figure.3.7. Conversion of Rweq to Rw using SP-2 chart

3.6.6. Saturation of water and saturation of hydrocarbons

Water saturation indicates about the amount of pore spaces filled with water. Hydrocarbon saturation can be determined by water saturation. Three equations are determined to calculate saturation of water, and are as follows:

1. Archie's Equation.
2. Indonesian Equation.
3. Simandoux Equation.

For clean lithology, Archie's equation is used, while for all rocks, Indonesian and Simandoux equations are used. Clean lithology is used in this field of interest, so Archie's is used to measure water saturation and the equation is:

$$S_w = \sqrt{\frac{R_w}{R_t} * \frac{1}{\phi_e^2}}$$

Where;

S_w = Saturation of water

R_w = Resistivity of water (calculated above)

R_t = Resistivity of true zone (calculated from LLD)

ϕ_e = Effective porosity

The number of pores that are filled with hydrocarbons represents the saturation of hydrocarbons. Water saturation and hydrocarbon saturation have an inverse relation. Hydrocarbon saturation can be determined using the following equation:

$$S_h = 1 - S_w$$

Where;

S_h = Saturation of hydrocarbons

S_w = Saturation of water

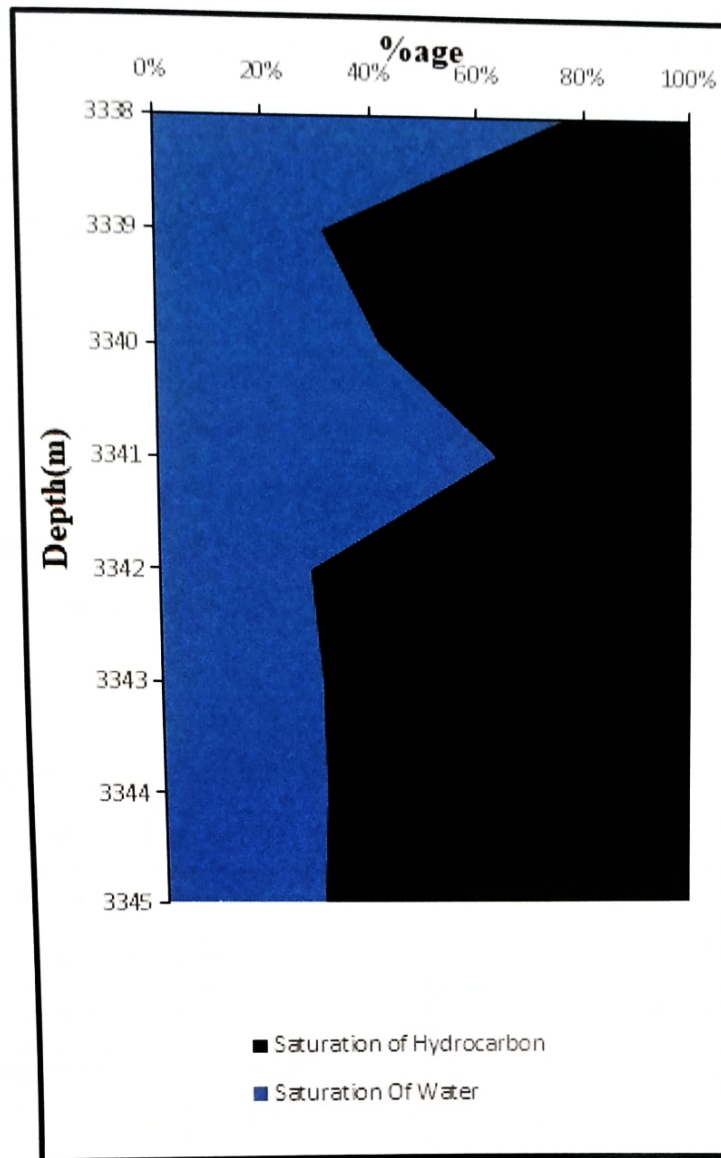


Figure.3.8.Cross plot between the saturation of water and hydrocarbons

Table 3.6. Average hydrocarbons and water saturation in %

Formation	Depth interval (m)	Avg. Saturation of Water (%)	Avg. Saturation of Hydrocarbon (%)
Lower Goru	3338-3345	41.37	58.62

Figure 3.8 shows the plot between the saturation of water and saturation of hydrocarbon of the desire depth of the zone of interest from 3338m to 3345m. From

3338m to 3339m the saturation of water decreases and then after 3339m the saturation of water again increases till 3341m, and then gradually decreases. The maximum saturation of water is at 3338m which is 77% and at 3341m which is 63.1%. Figure 3.8 shows that most of the zone of interest is saturated with hydrocarbon.

3.7. Result

Table 3.7 is showing numerous parameters that have been used in the zone of interest. It is interpreted from the parameters that B-interval has overall clean lithology. A great portion of zone of interest contain hydrocarbons. So, overall Formation is hydrocarbon saturated.

Table 3.7. Summary of different petrophysical parameters

Formation	Lower Goru
Thickness (m)	7
Avg. volume of shale (%)	9.43
Avg. volume of clean (%)	90.56
Average total porosity (%)	13.37
Avg. Effective porosity (%)	12.02
Resistivity of water (ohm.m)	0.05
Avg. water saturation (%)	41.37
Avg. hydrocarbon saturation (%)	58.62

CONCLUSION

Based on logs response, one zone of interest has been marked in Miano-09 well within B-interval of Goru formation. The thickness of the marked zone is 8m. There are no undulations in the GR curve. Gamma-ray response in this formation is low. The borehole profile at the zone of interest is almost gauged. There is a clear separation between MSFL and LLD in the marked zone of interest that shows the presence of formation fluid. The average volume of clean of prospect zone within B-interval is 90.56%. The average effective porosity is 12.02% which is calculated by the Gamma ray neutron tool. The average water saturation is 41.37% and the average hydrocarbon saturation is 58.62%. Based on the petrophysical analysis, the prospect zone has clean lithology and good effective porosity. Therefore, petrophysical analysis reveal that in Miano-09, B-interval of Lower goru formation is acting as an effective reservoir.

REFERENCES

- Ahmed, A., Ahmed, N., Ali, S. M. and Wali, N., 2007. Source potential and maturity trends of Lower Permian sediments in the Pujab Platform and adjoining areas, Pakistan.
- Ahmed, R, Ali. M and Ahmed, J., 1994 Review of Petroleum occurrence and Prospects of Pakistan with special references to adjoining Basins of India, Afghanistan and Iran. Pakistan Journal of Hydrocarbon Research.
- Kazmi A.H and Jan M.Q. (1997). Geology and Tectonics of Pakistan. Karachi, Pakistan: Graphic Publishers.
- Kazmi, A., H. and Abbasi, I. A., 2008. Stratigraphy and Historical Geology of Pakistan: National Center vof Excellence in Geology, University of Peshawar, Pakistan.
- Kadri, I.B. (1995). Petroleum Geology of Pakistan. Pakistan: PPL.
- Muhammad Yasin Khan, Muhammad Tayyab Raza and Umair Khan. (2020). Reservoir Characterization of the B-Interval of Lower Goru Formation, Miano 9 and 10, Miano area, Lower Indus Basin. Environmental and Earth Sciences Research Journal.
- Jadoon S.K., Jadoon, et al. 2019. "Interpretation of the Eastern Sulaiman fold-and-thrust belt, Pakistan: A passive roof duplex." Journal of Structural Geology 126 (2019)
- Shah, S.M.I., Ahmed ,R., Cheema, M.R., Fatmi, A.N., and Raza S.M.,. (1977 and 1980). Stratigraphy of Pakistan. Pakistan: Memoris, V (12).
- Shahzad and Raza, 2010. 2-D interpretation; Seismic modeling and estimation of rock properties of Miano block, Pakistan; unpublished B.S Thesis, Department of Earth and Environmental Sciences, Bahria University, Islamabad.

APPENDIX

Petrophysical parameters of B-interval of Miano-09 well.

Depth(m)	Caliper(IN)	GR(GAPI)	Vshale %	Vclean %	NPHI%	PHID %	PHIA %	PHIE %	R _w	Sw %	SH %
3338	6	40	18.367347	81.632653	3	12.90322581	7.951612903	6.491112574	0.05	77.0284	22.9716
3339	5.9	30	8.1632653	91.836735	3	32.25806452	17.62903226	16.18992758	0.05	30.8834	69.1166
3340	5.9	35	13.265306	86.734694	3	27.09677419	15.0483871	13.05217248	0.05	41.55064	58.44936
3341	6	55	33.673469	66.326531	6	27.74193548	16.87096774	11.18992758	0.05	63.19136	36.80864
3342	6	22	0	100	3	29.03225806	16.01612903	16.01612903	0.05	27.9227	72.0773
3343	6	23	1.0204082	98.979592	3	20.64516129	11.82258065	11.70194207	0.05	30.21322	69.78678
3344	6	23	1.0204082	98.979592	2	20	11	10.8877551	0.05	30.61543	69.38457
3345	6	22	0	100	2	19.35483871	10.67741935	10.67741935	0.05	29.6165	70.3835
Average	5.97	31.25	9.43	90.56	3.12	23.62	13.37	12.02	0.05	41.37	58.62

PETROPHYSICAL ANALYSIS OF MIANO-09 WELL, LOWER INDUS BASIN, PAKISTAN

by Umer Azam, Muhammad Awais, Usama Aman Ulah

Submission date: 18-Feb-2021 09:48PM (UTC-0800)

Submission ID: 1512881528

File name: Final_Thesis_-_Copy.docx (113.72K)

Word count: 5308

Character count: 28134

PETROPHYSICAL ANALYSIS OF MIANO-09 WELL, LOWER INDUS BASIN, PAKISTAN

ORIGINALITY REPORT



15%

SIMILARITY INDEX

8%

INTERNET SOURCES

4%

PUBLICATIONS

12%

STUDENT PAPERS

PRIMARY SOURCES

1	www.slb.com Internet Source	3%
2	Submitted to Higher Education Commission Pakistan Student Paper	3%
3	pubs.usgs.gov Internet Source	2%
4	www.iieta.org Internet Source	1%
5	Submitted to University of Portsmouth Student Paper	1%
6	Submitted to Indian School of Mines Student Paper	1%
7	Saif-Ur-Rehman K. Jadoon, Ding Lin, Siddique Akhtar Ehsan, Ishtiaq A. K. Jadoon, Muhammad Idrees. "Structural styles, hydrocarbon prospects, and potential of Miano and Kadanwari fields, Central Indus Basin,	1%

